Inhibition of cell membrane ingression at the division site by cell wall in fission yeast

Ting Gang Chew[1,2,*], Tzer Chyn Lim[1*], Yumi Osaki[3], Junqi Huang[1], Anton Kamnev[1], Tomoyuki Hatano[1], Masako Osumi[3,4], Mohan K. Balasubramanian[1]

Affiliations

[1]Division of Biomedical Sciences, Warwick Medical School, University of Warwick, Gibbet Hill Rd, Coventry, West Midlands, CV4 7AL, United Kingdom.

[2]ZJU-UoE Institute, Zhejiang University School of Medicine, International Campus, Zhejiang University, 718 East Haizhou Road, Haining, Zhejiang 314400, P.R. China.

[3]Integrated Imaging Research Support, 1-7-5-103, Hirakawa-cho, Chiyoda-ku, Tokyo 102-0093, Japan.

[4]Laboratory of Electron Microscopy/Bio-imaging Center, Japan Women's University, 2-8-1 Mejirodai, Bunkyo-ku, Tokyo 112-8681, Japan.

*Co-first authors

[#]Correspondence to: Mohan K. Balasubramanian (m.k.balasubramanian@warwick.ac.uk)

Total Characters: 19999

Abstract

Eukaryotic cells assemble an actomyosin ring during cytokinesis to function as a force-generating machine to drive membrane invagination, and to counteract the intracellular pressure and the cell surface tension. How the extracellular matrix affects actomyosin ring contraction has not been fully explored. While studying the *S. pombe* 1,3– β-glucan-synthase mutant *cps1*-191, which is defective in division septum synthesis and arrests with a stable actomyosin ring and, we found that weakening of the extracellular glycan matrix caused the generated spheroplasts to divide at the non-permissive condition. This non-medial slow division was dependent on a functional actomyosin ring and vesicular trafficking, but independent of normal septum synthesis. Interestingly, the high intracellular turgor pressure appears to play minimal roles in inhibiting ring contraction in the absence of cell wall remodeling in *cps1*-191 mutants as decreasing the turgor pressure alone did not enable spheroplast division. We propose that during cytokinesis, the extracellular glycan matrix restricts actomyosin ring contraction and membrane ingression, and remodeling of the extracellular components through division septum synthesis relieves the inhibition and facilitates actomyosin ring contraction.

Introduction

Animal cells and fungal cells require assembly and contraction of an actomyosin ring during cytokinesis. In fission yeast, the actomyosin ring contracts to drive membrane ingression, and coordinates with the septum assembly machinery to deposit cell wall materials at the division site (Ramos *et al.*, 2019). The fungal cell wall has been suggested as a functional equivalent of the extracellular matrix (ECM) in animal cells (Munoz *et al.*, 2013). The division septum is a special wall structure composed of primary and secondary septa. The primary septum is a structure that must be degraded to permit cell separation and the secondary septum is a structure that forms the cell wall once both cells are separated. The septum assembly machinery consists of α-glucan synthase Ags1 and β-glucan synthase Bgs1 and Bgs4. The β-glucan synthase Cps1/Bgs1 is essential for primary septum formation. Cps1 synthesizes specifically the linear β-glucan matrix of the primary septum at the division site and couples the extracellular glycan matrix to the

actomyosin ring via intermediate protein complexes (Munoz *et al.*, 2013; Cortes *et al.*, 2015; Davidson *et al.*, 2016; Sethi *et al.*, 2016). The β-glucan synthases Bgs4 and the α-glucan synthase Ags1 are primarily involved in the secondary septum formation and participate in the synthesis of primary septum (Garcia Cortes *et al.*, 2016). The deposition of extracellular glycan matrix coordinates with actomyosin ring contraction and stabilizes the contracting actomyosin ring at the division site (Munoz *et al.*, 2013; Arasada and Pollard, 2014).

How the extracellular glycan matrix influences actomyosin ring contraction (apart from its roles in ring stability during cytokinesis) has not been examined closely (Mishra *et al.*, 2012; Munoz *et al.*, 2013). In this study, we used the thermosensitive allele of β-1,3-glucan synthase, *cps1*-191 to address this question. The *cps1*-191 mutant is defective in β−1,3-glucan and septum synthesis and arrests with a non-contracting actomyosin ring at the non-permissive temperature (Liu *et al.*, 2000). Interestingly, we found that weakening of the extracellular glycan matrix in *cps1*-191 mutant at the non-permissive temperature has enabled actomyosin ring contraction and membrane ingression.

Results and discussion

Under the restrictive temperature, the β-glucan synthase mutant *cps1*-191 assembles actomyosin rings that do not contract (Liu *et al.*, 2000). It has been suggested that β-glucan synthesis at the division site is required to overcome the high intracellular turgor pressure during cytokinesis, and that the actomyosin ring may not be able to overcome the high turgor (Proctor *et al.*, 2012). To test if the turgor pressure inhibited ring contraction in *cps1*-191 mutants, we cultured *cps1*-191 cells in EMMA medium containing 0.8 M sorbitol to decrease the turgor pressure to that inside the cells at the restrictive temperature, and we added 2-deoxyglucose (2-DG) to this culture to prevent further glucan synthesis at the division site and elsewhere in the cell (Megnet, 1965; Svoboda and Smith, 1972; Osumi *et al.*, 1998). A recent study showed that rings in *cps1*-191 mutant cells constricted slowly after shifting to the restrictive temperature for ~2 hours prior to microscopy at the restrictive temperature (Dundon and Pollard, 2020). To ensure a highly penetrant phenotype for *cps1*-191, we shifted the *cps1*-191 cells to the restrictive temperature for ~6 hours prior to microscopy, which

was performed at the restrictive temperature. As previously reported, actomyosin rings of *cps1*-191 cells maintained in normal turgor pressure did not undergo contraction (Figure 1A). We occasionally observed that parts of the *cps1*-191 cells swelled into a bump and the cells lysed eventually with a collapsing ring (Figure 1B). Culturing *cps1*-191 cells in EMMA medium containing 0.8 M sorbitol, did not increase actomyosin ring contraction events and phenotypically these cells resembled *cps1*-191 grown under normal growth conditions in EMMA medium, in which a high intracellular turgor pressure is maintained (Figure 1C and 1D). Thus, our results showed that a decreased turgor pressure does not allow ring contraction in *cps1*-191 mutant cells.

Next, we considered the possibility that the extracellular glycan matrix inhibited ring contraction and membrane ingression in *cps1*-191 mutants in the absence of cell wall remodeling. The Cps1 is a transmembrane protein that (along with other integral membrane proteins, such as Ags1 and Bgs4) links actomyosin rings underneath the cell membrane to the extracellular glycan matrix (Cortes *et al.*, 2005; Cortes *et al.*, 2012; Munoz *et al.*, 2013; Arasada and Pollard, 2015; Davidson *et al.*, 2016; Sethi *et al.*, 2016; Martin-Garcia *et al.*, 2018). It was possible that in the absence of division septum synthesis (and thereby cell wall remodeling), the actomyosin rings are stably fixed to the inactive *cps1*-191 gene-product or other integral membrane proteins (such as mok1, sbg1, and bgs4) that link the cell wall to the actomyosin ring. To test if this was the case, we weakened the extracellular glycan matrix by treating the *cps1*-191 cells with cell wall lytic enzymes and further blocking new cell wall and septum synthesis by supplementing the culture with 2-DG. Interestingly, upon weakening of the cell wall, myosin rings in *cps1*-191 mutant expressing the regulatory light chain of myosin tagged with the fluorescent protein tdTomato (Rlc1-tdTomato) underwent contraction coupled with membrane ingression at the restrictive temperature of 36 ºC (Figure 2A; GFP-tagged Syntaxin-like protein Psy1 was used as a cell membrane marker; n = 19/29 spheroplasts). Consistently, contracting actin rings labeled with the Lifeact-mCherry were also detected in the *cps1*-191 mutant upon weakening of cell wall, suggesting that the actomyosin rings were driving the contraction and membrane ingression (Figure 2B; n = 5/41 spheroplasts). These mutant spheroplasts with weakened cell wall often divided non-medially into two, and the rings contracted at much reduced rate (0.061 ± 0.021 μm/min, $n_{spheroplast}$ = 8) compared to wild-type cells

(0.299 ± 0.059 μm/min, n_{cell} = 14) (Figure 2C). The slow rate of ring contraction is comparable to that of in the wild-type spheroplasts in which the rings slide along the cell membrane during ring contraction (0.046 ± 0.031 μm/min, $n_{wild\text{-}type\ spheroplast}$ = 40). We frequently observed that the rings contracted till mid-phase of division and disassembled before completion of cytokinesis. The spheroplasts however went on to divide into two entities (Figure 2A and 2B). The segregation of daughter nuclei in the *cps1*-191 spheroplasts was often not coordinated with the cytokinesis, with some spheroplasts have two nuclei in one of the daughter entities or have cleaved nuclei, presumably due to the non-medial division (Supplementary figure 1). The mis-coordination of cytofission and nuclear division spatially could arise from the variable dumb-bell shaped morphology of *cps1*-191 spheroplasts (Mishra *et al.*, 2012). The functions of Mto1 and Mto2, which are involved in the assembly of post-anaphase microtubule arrays may also contribute to this mis-coordination defects (Dundon and Pollard, 2020). Since the *cps1*-191 mutant spheroplast division was morphologically different from normal fission yeast cell division and was mimicking the morphological changes of some animal cells during division, we have called this type of division as cytofission.

Analysis of the extracellular glycan matrix using calcofluor staining (a division septum-specific fluorochrome) (JC *et al.*, 2018) in cells undergoing cytofission in EMMA containing sorbitol and 2-DG medium revealed that the division site of *cps1*-191 spheroplasts undergoing cytofission with 2-DG medium contained significantly reduced β-glucan materials (Figure 2D). Further study with the high-resolution scanning electron microscopy showed that the glucan fibrils regenerated in *cps1*-191 spheroplasts without 2-DG (Figure 2E; bottom panel) while the fibrils were not noticeable in *cps1*-191 spheroplasts with 2-DG (Figure 2E; top panel). The glucan fibrils commonly present at the division site of fission yeast was largely absent in *cps1*-191 spheroplasts undergoing cytofission (Supplementary figure 2). Taken together, we showed that weakening of cell wall in *cps1*-191 cells at non-permissive temperature and ensuing further inhibition of new cell wall and septum synthesis with 2-DG facilitates a novel cytofission event that leads to division of one spheroplast into two in the absence of detectable division-septum growth. Our results also suggested that the extracellular glycan matrix anchored to the actomyosin rings negatively

regulates the ring contraction and membrane ingression. This is consistent with a previous finding that the absence of the Bgs4-synthesized β-glucan in the septum promoted a faster ring contraction and membrane ingression than that of normal septa, and at the same time, the synthesis and ingression of septum wall progressed slower than that of a normal septum (Munoz *et al.*, 2013).

A reduction of β-glucan may result in an increased amount of α-glucan in the cell wall of fission yeast. To test if the cytofission of *cps1*-191 spheroplasts were due to the synthesis of α-glucan at the division site, we prepared the *cps1*-191 *mok1*-664 double mutant spheroplasts containing the thermosensitive alleles of both α- and β- glucan synthases, and imaged the myosin rings and cell membrane in this double mutant spheroplasts at the non-permissive temperature. Similar to the *cps1*-191 spheroplast, the *cps1*-191 *mok1*-664 double mutant spheroplasts underwent cytofission (Figure 3A, n = 11/26), suggesting that α-glucan and β-glucan synthesis did not contribute significantly to the cytofission events.

Normal fission yeast cells that just complete ring contraction and membrane ingression are not entirely separated until the primary septum digestion of the division septum connecting the two newly-divided cells (Sipiczki, 2007). This process is achieved in fission yeast through the action of endoglucanases (Martin-Cuadrado *et al.*, 2003; Dekker *et al.*, 2004; Garcia *et al.*, 2005). We tested if proteins involved in the separation of fission yeast cells were also involved in the cytofission, which would be expected if trace amounts of division septum had been deposited during ring contraction. To this end, we constructed double mutant spheroplasts of *cps1*-191 lacking the endoglucanases *eng1* (β-glucanase) and *agn1* (α-glucanase), respectively. Similar to the single mutant *cps1*-191, the double mutants lacking either of the two endoglucanases underwent cytofission upon weakening of the cell wall (Figure 3B, n = 8/23; Figure 3C, n = 11/38). The results indicated that the cytofission events of *cps1*-191 mutants does not require the break-down of cell wall materials by endoglucanases, even though cytofission leads to the complete separation of spheroplasts.

In ~53% of the *cps1*-191 spheroplasts (53 out of 99 spheroplasts) that underwent cytofission, the rings contracted till mid-phase of division and disassembled before division into two entities. We tested if the ESCRT abscission complex was involved in the cytofission by removing two of the ESCRT proteins Vps4 and Vps20 in the *cps1*-191 spheroplasts. The *cps1*-191 *vps4*Δ and *cps1*-191 *vps20*Δ double mutant spheroplasts underwent cytofission like in the single *cps1*-191 mutant spheroplast (Supplementary figure 3A, n = 14/14; Supplementary figure 3B, n = 8/8). It is possible that the completion of cytofission without the actomyosin rings was achieved via an unknown cell abscission mechanism.

Previous studies suggested under certain circumstances, some eukaryotic cells are able to divide without an actomyosin ring (Proctor *et al.*, 2012; Choudhary *et al.*, 2013; Flor-Parra *et al.*, 2014; Dix *et al.*, 2018; Ramos *et al.*, 2019). To see if the cytofission was driven by contraction of the actomyosin ring, we first perturbed the functions of rings using Latrunculin-A (LatA) to inhibit actin polymerization (Morton *et al.*, 2000; Fujiwara *et al.*, 2018). *cps1*-191 spheroplasts treated with DMSO underwent ring contraction, membrane ingression, and completed cytofission (Figure 4A; n = 11/16 spheroplasts). By contrast, *cps1*-191 spheroplasts treated with LatA underwent ring disassembly and failed to divide into two entities or ingressed very slowly resembling dividing cells after long time incubation with LatA (Ramos *et al.*, 2019). Interestingly, the smaller entity retracted into the bigger entity, probably due to the imbalance of intracellular pressures (Figure 4B; n = 27/33 spheroplasts).

Next, we perturbed the myosin component of actomyosin rings by deleting *rlc1*, the regulatory light chain of myosin II (Le Goff *et al.*, 2000; Naqvi *et al.*, 2000; Pollard *et al.*, 2017), in *cps1*-191 mutants. It has been shown that the cells lacking *rlc1* (*rlc1*Δ) is cold sensitive and fail to undergo cytokinesis at low temperature, but at high temperatures, the *rlc1*Δ cells assemble an intact actomyosin ring that contracts normally (Naqvi *et al.*, 2000) (Supplementary figure 4; n = 31/31 cells). We used this differential temperature requirement to test the essentiality of actomyosin ring functions in cytofission. If the actomyosin ring was essential in driving cytofission, the absence of

rlc1 might render the cells with weakened cell wall unable to undergo cytofission at the high temperature, which is normally permissive for cell division in *rlc1*Δ cells alone (Naqvi *et al.*, 2000). Consistent with the LatA experimental findings, the double mutant *cps1*-191 *rlc1*Δ with weakened cell wall did not undergo ring contraction at the high temperature (Figure 4C; n = 23/24 spheroplasts), whereas the single mutant of *cps1*-191 could undergo cytofission.

Targeted membrane deposition is required in the cytokinesis of fission yeast (Wang *et al.*, 2016; Onwubiko *et al.*, 2019). Next, we tested if targeted membrane deposition at the division site facilitates actomyosin ring contraction in cytofission. When the vesicular trafficking across the endomembrane system was inhibited using brefeldin A in the *cps1*-191 spheroplasts, the myosin rings were not able to contract to drive cytofission events (Figure 4D, n = 27/27). This result suggested that addition of cell membrane via targeted membrane trafficking at the division site is required to enable cytofission.

Our study reveals that the extracellular glycan matrix inhibits actomyosin ring contraction in the absence of cell wall remodeling and division septum synthesis. When the inhibition is relieved by experimental treatments like ones reported in this study, or by septum synthesis, the actomyosin ring contracts to drive the membrane ingression. A previous study by Proctor *et al*. analyzed *cps1*-191 mutants and explained that the failure of membrane ingression in the mutant was due to a defect in division-septum assembly. The authors also proposed that the high intracellular turgor pressure prevents actomyosin ring contraction in fission yeast (Proctor *et al.*, 2012). We tested this model by lowering the turgor pressure in *cps1*-191 mutant cells and found that it was not sufficient to enable membrane ingression in the absence of cell wall remodeling in the *cps1*-191 cells. However, the ability of *cps1*-191 mutant cells to divide upon weakening of cell wall indicates that the actomyosin ring in *cps1*-191 mutant cells is capable of driving membrane ingression even when the division septum assembly is defective. When cell wall remodeling is normal, like in wild-type cells, ring contraction and membrane ingression coordinate with cell wall and septum growth. The lowering of turgor pressure by sorbitol addition in wild type cells with normal cell wall remodeling may facilitate ring contraction, explaining the findings of Proctor et al (Proctor *et al.*,

2012). The fact that ring contraction is slower during cytofission however, agrees better with the work of O' Shaughnessy and colleagues, who have proposed that the rate of septum synthesis sets the rate of cytokinesis (Stachowiak *et al.*, 2014). It is possible that our work reveals the highest rate of actomyosin ring contraction when confronted with membrane drag and viscous drag of the cytosol. The slow ring contraction rate could be as a result of a reduced amount of Cps1-191 or cytokinetic proteins at the division site (Cortes *et al.*, 2015). In fission yeast spheroplasts, the actomyosin ring is probably required at the early phase of cytofission to drive spheroplasts into a dumbbell shape with high curvature. Although we cannot exclude the possibility that residual and undetectable actomyosin structures may facilitate division after seeming actomyosin ring disassembly, recent work suggests other potential mechanisms not involving actomyosin rings or ESCRT in division of dumbbell shaped vesicles. It has been proposed that the spontaneous curvature in dumbbell-shape lipid vesicles generates constriction forces to induce membrane fission. This leads to the division of a dumbbell-shaped lipid vesicle into two with an increased curvature (Steinkuhler *et al.*, 2020).

The yeast cell wall consists of mainly glycan matrix and glycosylated proteins and has been suggested as a functional equivalent of the extracellular matrix (ECM) in animal cells (Munoz *et al.*, 2013). The mechanical interaction between the cytokinetic actomyosin ring and the ECM is not well understood. A recent study of zebrafish epicardial cells in the heart explants shows the cell-ECM adhesions at the division site. The cell-ECM adhesions lead to the traction forces at the cytokinetic ring that inhibit cytokinesis (Uroz *et al.*, 2019). An early biophysical study also detected a large traction force at the cleavage furrow of the fibroblast cells cultured on an elastic substrate, suggesting an interaction of cytokinetic machinery and ECM (Burton and Taylor, 1997). When the cell-ECM adhesion is enhanced during mitosis, the cleavage furrow ingression is inhibited in the epithelial cells (Taneja *et al.*, 2016). Consistently, our study shows that the anchoring of actomyosin rings to the extracellular glycan matrix that do not undergo remodeling (due to a defective Bgs1) prevents the actomyosin ring contraction and cell membrane ingression. Weakening of the extracellular glycan matrix, presumably mimicking a decreased cell-ECM adhesion, has enabled cytofission events.

Materials and methods

Yeast strains, medium, and culture conditions

Table S1 lists the *S. pombe* strains used in our study. Standard fission yeast genetic techniques were used to prepare the strains. The rich medium YEA (5 g/l yeast extract, 30 g/l glucose, 225 mg/l adenine) was used to culture cells until mid-log phase at 24°C before the temperature shift. Latrunculin-A (latA) (Enzo Life Sciences; BML-T119) was used at the final concentration of 150 µM to perturb the actin dynamics in spheroplasts. Brefeldin A (Fisher Scientific; 15526276) was used at the final concentration of 75 μ M to slow down plasma membrane invagination. Calcofluor White Stain for cell wall staining was purchased from Sigma.

Preparation of *S. pombe* spheroplasts for live-cell imaging (spheroplasting)

The *cps1*-191 cells used in this study were first cultured in YEA medium at 24°C to mid-log phase (OD_{595} = 0.2-0.5), and then were shifted to 36°C for 6 hours 15 minutes (non-permissive conditions). Twenty milliliters of culture were spun down at 3,000 r.p.m. for 1 minute and washed once with equal volume of E-buffer (50 mM sodium citrate, 100 mM sodium phosphate, [pH 6.0]). After spinning down the cells and resuspending cells in 5 ml of E-buffer containing 1.2 M sorbitol, the cell suspension was incubated with 30 mg of lysing enzyme Enzymes from Trichoderma harzianum or Glucanex (Sigma, L1412; an enzymatic mixture of at least glucanases, cellulase, protease, and chitinase activities) at 36°C with shaking at 80 r.p.m. for 90 minutes. This was followed by continuous incubation with 40 µl of LongLife Zymolyase (G-Biosciences, 1.5 U/µl; an enzymatic mixture with at least β-glucanase, protease and mannanase activities) at 36°C with shaking at 80 r.p.m. for 60 minutes. After enzymatic digestion, the cell suspensions were spun down at 450 xg for 2 minutes and washed once with 5 ml of E-buffer containing 0.6 M sorbitol. After spinning at 450 xg for 2 minutes, the spheroplasts were recovered in 10 ml EMMA medium (Edinburgh minimal medium with all amino acids and nucleotides supplements) containing 0.8 M sorbitol and 0.5% (v/v) of 1 M 2-deoxyglucose (Sigma, D6134) for 30 minutes at 36°C prior to microscopy imaging.

Sample preparation for light microscopy

One to two milliliters of spheroplast suspensions in EMMA medium containing 0.8 M sorbitol and 0.5% (v/v) of 1 M 2-deoxyglucose (Sigma, D6134) were concentrated to 20-100 µl by centrifugation at 450 xg for 2 minutes. About 10 µl of concentrated spheroplasts were loaded onto an Ibidi µ-Slide 8-Well glass bottom dish (Cat. No. 80827), and covered with mineral oil (Sigma, M5310) to prevent evaporation during imaging process.

To image cells in Figure 1 and supplementary Figure 4, the *cps1*-191 cells and *rlc1*Δ cells after shifting to non-permissive conditions were treated with buffers used to prepare spheroplasts but with the lysing and lytic enzymes omitted to preserve the cell wall integrity. After the buffer washing, the *cps1*-191 cells in the Figure1 were recovered in EMMA medium with full supplements containing 0.8 M sorbitol and 0.5% 2-DG. For the *rlc1*Δ cells in the supplementary Figure 4, after the buffer washing, the cells were recovered in EMMA medium with full supplements containing 0.8 M sorbitol but not 2-DG to allow septation.

Sample preparation for electron microscopy

Two hundred and fifty milliliters of cells with OD_{595} 0.2 were collected for spheroplasting. Spheroplasts were prepared with the spheroplasting method described above. Spheroplasts were spun down from EMMA with 0.8 M sorbitol and resuspended in phosphate-buffered saline (PBS) with 2.5% glutaraldehyde and 1.2 M sorbitol. Fixation solution was prepared by adding 2% glutaraldehyde and dissolving 1.2 M sorbitol in PBS. After 2 hours incubation at room temperature, spheroplasts were spun down in round bottom tubes. The following procedures were done at 4°C and gently (vortex mixer was avoided). Spheroplasts were resuspended in fixation solution and stood on ice for 2 hours. The spheroplasts were separated into 2 tubes: washed and unwashed samples. Unwashed samples were stored at 4°C. The washed samples were washed with 1 mL PBS containing 1.2 M sorbitol for three times. Lastly the spheroplasts were resuspended in 1 mL PBS containing 1.2 M sorbitol and stored at 4°C before electron microscopy.

For electron microscopy, glutaraldehyde-fixed cells were placed on a slide glass whose surface was pre-treated with 0.1% poly-L-lysine. They were washed with 0.1 M phosphate buffer (pH 7.2), post-fixed with 1% osmium tetroxide at 4°C for 1 hour, dehydrated with graded series of ethanol, and critical point dried with a Leica EM CPD030 apparatus (Leica Microsystems, Vienna). The specimens were coated with osmium tetroxide by osmium coater (Vacuum Device.inc, Japan) and observed with S-3400N and SU8020 scanning electron microscope (Hitachi High Technologies, Tokyo) at 10.0 kV and 1.0 kV respectively (Namiki *et al.*, 2011).

Light microscopy

The Andor Revolution XD spinning disk confocal microscope was used to image the spheroplasts and cells at 36°C. The microscope was equipped with a Nikon ECLIPSE Ti inverted microscope, Nikon Plan Apo Lambda 100×/1.45N.A. oil immersion objective lens, a spinning-disk system (CSU-X1; Yokogawa), and the Andor iXon Ultra EMCCD camera 897 or 888. The Andor IQ3 software was used to acquire images at the pixel size of 80 nm/pixel or 69 nm/pixel, depending on the camera models. Laser lines at wavelengths of 405 nm, 488 nm or 561 nm were used for the excitation of fluorophores. Most images were acquired with Z-step sizes of 0.5 µm as listed here: Figure 2A (12 µm / 25 Z-sections); Figure 2B (10 µm / 21 Z -sections); Figure 3A (10 µm / 21 Z -sections); Figure 3B (15 µm / 31 Z-sections); Figure 3C (15 µm / 31 Z-sections); Figure 4A (15 µm / 31 Z-sections); Figure 4B (12 µm / 25 Z-sections); Figure 4C (13 µm / 27 Z-sections); Figure 4D (10 µm / 21 Z-sections); Supplementary figure 1 (10 µm / 21 Z-sections); Supplementary figure 3A (15 µm / 31 Z-sections); Supplementary figure 3B (13 µm / 27 Z-sections); Supplementary figure 4 (13 µm / 27 Z-sections).

Image analysis

Images were processed using Fiji. The time-lapse montages are maximum intensity projections of Z-stack of specified time points. All images analyzed were prepared in this study, except images for quantification of the rate of ring sliding in wild-type spheroplasts in which the data was based on the time-lapse images acquired in a previous study (Lim *et al.*, 2018).

Acknowledgements

This work was supported by research grants from Wellcome Trust (WT101885MA) and ERC (GA 671083 - ACTOMYOSIN RING) to MKB. Part of the work was supported by the Fundamental Research Funds for the Central Universities (K20200099) to TGC.

Figure Legends

Figure 1. Lowering down turgor pressure does not allow cell membrane ingression in *cps1* mutant cells.

(A) *cps1*-191 GFP-*psy1 rlc1*-tdTomato cells were cultured in YEA at the restrictive temperature of 36°C for 6.5 hours and were processed similarly using the spheroplasting protocol but omitting lysing enzymes and Zymolyase. Cells in the EMMA medium with 2-DG were imaged at 36°C. Green: GFP-*psy1*. Red: *rlc1*-tdTomato.

(B) Some *cps1*-191 GFP-*psy1 rlc1*-tdTomato cells lysed after more than 6.5 hours of incubation at the restrictive temperature. Treatment of cells was same as in Figure 1(A). Green: *rlc1*-tdTomato. Red: GFP-*psy1*.

(C) *cps1*-191 GFP-*psy1 rlc1*-tdTomato cells were cultured in YEA at the restrictive temperature for 6.5 hours and were processed similarly using the spheroplasting protocol but omitting lysing enzymes and Zymolyase. Cells were imaged at 36°C in the EMMA medium containing 2-DG and 0.8 M sorbitol to lower down the turgor pressure. Green: GFP-*psy1*. Red: *rlc1*-tdTomato.

(D) *cps1*-191 GFP-*psy1 rlc1*-tdTomato cells treated as in Figure 1(C) were stained with calcofluor dye to reveal the cell wall.

Scale bar: 5 μm

Figure 2. Weakening of cell wall allows ring contraction and cell membrane ingression.

(A) Two examples of *cps1*-191 spheroplasts underwent cytofission at 36°C. The *cps1*-191 GFP-*psy1 rlc1*-tdTomato cells were cultured at 36°C for 6.5 hours, processed into spheroplasts, and recovered for 1 hour at 36°C prior to imaging.

(B) Two examples of *cps1*-191 spheroplasts expressing Lifeact-mCherry underwent cytofission at 36°C. The *cps1*-191 GFP-*psy1 lifeact*-mCherry cells were cultured at 36°C for 6.5 hours, processed into spheroplasts, and recovered for 1 hour at 36°C prior to imaging.

(C) Quantification of the rate of ring contraction in wild type cells and *cps1*-191 spheroplasts undergoing cytofission.

(D) Wild type cells and *cps1*-191 GFP-*psy1 rlc1*-tdTomato spheroplasts were stained with the calcofluor dye. The image was pseudo-colored in green to represent calcofluor staining.

(E) Electron micrographs of *cps1*-191 GFP-*psy1 rlc1*-tdTomato spheroplasts regenerated in medium with or without 2-DG.

Scale bar: 5 μm except Figure 2E, which is 1 μm; Error bars: standard deviation

Figure 3. The *cps1*-191 mutant spheroplasts undergo cytofission independent of the α-glucan synthase and endoglucanases.

(A) Cytofission in *cps1*-191 *mok1*-664 GFP-*psy1 rlc1*-tdTomato.

(B) Cytofission in *cps1*-191 *agn1*Δ GFP-*psy1 rlc1*-tdTomato.

(C) Cytofission in *cps1*-191 *eng1*Δ GFP-*psy1 rlc1*-tdTomato.

Scale bar: 5 μm

Figure 4. The function of actomyosin rings is required in the *cps1*-191 mutant spheroplasts to undergo cytofission.

(A) *cps1*-191 GFP-*psy1 rlc1*-tdTomato spheroplasts underwent cytofission in the presence of DMSO. Left panel shows the DIC images; right panel shows the fluorescence micrographs.

(B) *cps1*-191 GFP-*psy1 rlc1*-tdTomato spheroplasts were incubated with 150 μm Lat-A. Left panel shows the DIC images; right panel shows the fluorescence micrographs.

(C) *rlc1*Δ *cyk3*-GFP spheroplasts failed to undergo cytofission at 36°C. The *rlc1*Δ *cyk3*-GFP cells were cultured at 36°C for 6.5 hours, processed into spheroplasts, and then recovered in minimal medium containing sorbitol prior to imaging at 36°C. Top panel shows the DIC images; bottom panel shows the fluorescence micrographs.

(D) The *cps1*-191 GFP-*psy1* *rlc1*-tdTomato spheroplasts failed to undergo cytofission in the presence of 75 μM brefeldin A.

Scale bar: 5 μm

References

Arasada, R., and Pollard, T.D. (2014). Contractile ring stability in S. pombe depends on F-BAR protein Cdc15p and Bgs1p transport from the Golgi complex. Cell Rep *8*, 1533-1544.

Arasada, R., and Pollard, T.D. (2015). A role for F-BAR protein Rga7p during cytokinesis in S. pombe. J Cell Sci *128*, 2259-2268.

Burton, K., and Taylor, D.L. (1997). Traction forces of cytokinesis measured with optically modified elastic substrata. Nature *385*, 450-454.

Choudhary, A., Lera, R.F., Martowicz, M.L., Oxendine, K., Laffin, J.J., Weaver, B.A., and Burkard, M.E. (2013). Interphase cytofission maintains genomic integrity of human cells after failed cytokinesis. Proc Natl Acad Sci U S A *110*, 13026-13031.

Cortes, J.C., Carnero, E., Ishiguro, J., Sanchez, Y., Duran, A., and Ribas, J.C. (2005). The novel fission yeast (1,3)beta-D-glucan synthase catalytic subunit Bgs4p is essential during both cytokinesis and polarized growth. J Cell Sci *118*, 157-174.

Cortes, J.C., Pujol, N., Sato, M., Pinar, M., Ramos, M., Moreno, B., Osumi, M., Ribas, J.C., and Perez, P. (2015). Cooperation between Paxillin-like Protein Pxl1 and Glucan Synthase Bgs1 Is Essential for Actomyosin Ring Stability and Septum Formation in Fission Yeast. PLoS Genet *11*, e1005358.

Cortes, J.C., Sato, M., Munoz, J., Moreno, M.B., Clemente-Ramos, J.A., Ramos, M., Okada, H., Osumi, M., Duran, A., and Ribas, J.C. (2012). Fission yeast Ags1 confers the essential septum strength needed for safe gradual cell abscission. J Cell Biol *198*, 637-656.

Davidson, R., Pontasch, J.A., and Wu, J.Q. (2016). Sbg1 Is a Novel Regulator for the Localization of the beta-Glucan Synthase Bgs1 in Fission Yeast. PLoS One *11*, e0167043.

Dekker, N., Speijer, D., Grun, C.H., van den Berg, M., de Haan, A., and Hochstenbach, F. (2004). Role of the alpha-glucanase Agn1p in fission-yeast cell separation. Mol Biol Cell *15*, 3903-3914.

Dix, C.L., Matthews, H.K., Uroz, M., McLaren, S., Wolf, L., Heatley, N., Win, Z., Almada, P., Henriques, R., Boutros, M., Trepat, X., and Baum, B. (2018). The Role of Mitotic Cell-Substrate Adhesion Re-modeling in Animal Cell Division. Dev Cell *45*, 132-145 e133.

Dundon, S.E.R., and Pollard, T.D. (2020). Microtubule Nucleation Promoters Mto1 and Mto2 Regulate Cytokinesis in Fission Yeast. Mol Biol Cell, mbcE19120686.

Flor-Parra, I., Bernal, M., Zhurinsky, J., and Daga, R.R. (2014). Cell migration and division in amoeboid-like fission yeast. Biol Open *3*, 108-115.

Fujiwara, I., Zweifel, M.E., Courtemanche, N., and Pollard, T.D. (2018). Latrunculin A Accelerates Actin Filament Depolymerization in Addition to Sequestering Actin Monomers. Curr Biol *28*, 3183-3192 e3182.

Garcia Cortes, J.C., Ramos, M., Osumi, M., Perez, P., and Ribas, J.C. (2016). The Cell Biology of Fission Yeast Septation. Microbiol Mol Biol Rev *80*, 779-791.

Garcia, I., Jimenez, D., Martin, V., Duran, A., and Sanchez, Y. (2005). The alpha-glucanase Agn1p is required for cell separation in Schizosaccharomyces pombe. Biol Cell *97*, 569-576.

JC, G.C., Ramos, M., Konomi, M., Barragan, I., Moreno, M.B., Alcaide-Gavilan, M., Moreno, S., Osumi, M., Perez, P., and Ribas, J.C. (2018). Specific detection of fission yeast primary septum reveals septum and cleavage furrow ingression during early anaphase independent of mitosis completion. PLoS Genet *14*, e1007388.

Le Goff, X., Motegi, F., Salimova, E., Mabuchi, I., and Simanis, V. (2000). The S. pombe rlc1 gene encodes a putative myosin regulatory light chain that binds the type II myosins myo3p and myo2p. J Cell Sci *113 Pt 23*, 4157-4163.

Lim, T.C., Hatano, T., Kamnev, A., Balasubramanian, M.K., and Chew, T.G. (2018). Equatorial Assembly of the Cell-Division Actomyosin Ring in the Absence of Cytokinetic Spatial Cues. Curr Biol *28*, 955-962 e953.

Liu, J., Wang, H., and Balasubramanian, M.K. (2000). A checkpoint that monitors cytokinesis in Schizosaccharomyces pombe. J Cell Sci *113 (Pt 7)*, 1223-1230.

Martin-Cuadrado, A.B., Duenas, E., Sipiczki, M., Vazquez de Aldana, C.R., and del Rey, F. (2003). The endo-beta-1,3-glucanase eng1p is required for dissolution of the primary septum during cell separation in Schizosaccharomyces pombe. J Cell Sci *116*, 1689-1698.

Martin-Garcia, R., Arribas, V., Coll, P.M., Pinar, M., Viana, R.A., Rincon, S.A., Correa-Bordes, J., Ribas, J.C., and Perez, P. (2018). Paxillin-Mediated Recruitment of Calcineurin to the Contractile

Ring Is Required for the Correct Progression of Cytokinesis in Fission Yeast. Cell Rep *25*, 772-783 e774.
Megnet, R. (1965). Effect of 2-deoxyglucose on Schizosaccharomyces pombe. J Bacteriol *90*, 1032-1035.
Mishra, M., Huang, Y., Srivastava, P., Srinivasan, R., Sevugan, M., Shlomovitz, R., Gov, N., Rao, M., and Balasubramanian, M. (2012). Cylindrical cellular geometry ensures fidelity of division site placement in fission yeast. J Cell Sci *125*, 3850-3857.
Morton, W.M., Ayscough, K.R., and McLaughlin, P.J. (2000). Latrunculin alters the actin-monomer subunit interface to prevent polymerization. Nat Cell Biol *2*, 376-378.
Munoz, J., Cortes, J.C., Sipiczki, M., Ramos, M., Clemente-Ramos, J.A., Moreno, M.B., Martins, I.M., Perez, P., and Ribas, J.C. (2013). Extracellular cell wall beta(1,3)glucan is required to couple septation to actomyosin ring contraction. J Cell Biol *203*, 265-282.
Naqvi, N.I., Wong, K.C., Tang, X., and Balasubramanian, M.K. (2000). Type II myosin regulatory light chain relieves auto-inhibition of myosin-heavy-chain function. Nat Cell Biol *2*, 855-858.
Onwubiko, U.N., Mlynarczyk, P.J., Wei, B., Habiyaremye, J., Clack, A., Abel, S.M., and Das, M.E. (2019). A Cdc42 GEF, Gef1, through endocytosis organizes F-BAR Cdc15 along the actomyosin ring and promotes concentric furrowing. J Cell Sci *132*.
Osumi, M., Sato, M., Ishijima, S.A., Konomi, M., Takagi, T., and Yaguchi, H. (1998). Dynamics of cell wall formation in fission yeast, Schizosaccharomyces pombe. Fungal Genet Biol *24*, 178-206.
Pollard, L.W., Bookwalter, C.S., Tang, Q., Krementsova, E.B., Trybus, K.M., and Lowey, S. (2017). Fission yeast myosin Myo2 is down-regulated in actin affinity by light chain phosphorylation. Proc Natl Acad Sci U S A *114*, E7236-E7244.
Proctor, S.A., Minc, N., Boudaoud, A., and Chang, F. (2012). Contributions of turgor pressure, the contractile ring, and septum assembly to forces in cytokinesis in fission yeast. Curr Biol *22*, 1601-1608.
Ramos, M., Cortes, J.C.G., Sato, M., Rincon, S.A., Moreno, M.B., Clemente-Ramos, J.A., Osumi, M., Perez, P., and Ribas, J.C. (2019). Two S. pombe septation phases differ in ingression rate, septum structure, and response to F-actin loss. J Cell Biol *218*, 4171-4194.
Sethi, K., Palani, S., Cortes, J.C., Sato, M., Sevugan, M., Ramos, M., Vijaykumar, S., Osumi, M., Naqvi, N.I., Ribas, J.C., and Balasubramanian, M. (2016). A New Membrane Protein Sbg1 Links the Contractile Ring Apparatus and Septum Synthesis Machinery in Fission Yeast. PLoS Genet *12*, e1006383.
Sipiczki, M. (2007). Splitting of the fission yeast septum. FEMS Yeast Res *7*, 761-770.
Stachowiak, M.R., Laplante, C., Chin, H.F., Guirao, B., Karatekin, E., Pollard, T.D., and O'Shaughnessy, B. (2014). Mechanism of cytokinetic contractile ring constriction in fission yeast. Dev Cell *29*, 547-561.
Steinkuhler, J., Knorr, R.L., Zhao, Z., Bhatia, T., Bartelt, S.M., Wegner, S., Dimova, R., and Lipowsky, R. (2020). Controlled division of cell-sized vesicles by low densities of membrane-bound proteins. Nat Commun *11*, 905.
Svoboda, A., and Smith, D.G. (1972). Inhibitory effect of 2-deoxy-glucose on cell wall synthesis in cells and protoplasts of Schizosaccharomyces pombe. Z Allg Mikrobiol *12*, 685-699.
Taneja, N., Fenix, A.M., Rathbun, L., Millis, B.A., Tyska, M.J., Hehnly, H., and Burnette, D.T. (2016). Focal adhesions control cleavage furrow shape and spindle tilt during mitosis. Sci Rep *6*, 29846.
Uroz, M., Garcia-Puig, A., Tekeli, I., Elosegui-Artola, A., Abenza, J.F., Marin-Llaurado, A., Pujals, S., Conte, V., Albertazzi, L., Roca-Cusachs, P., Raya, A., and Trepat, X. (2019). Traction forces at the cytokinetic ring regulate cell division and polyploidy in the migrating zebrafish epicardium. Nat Mater *18*, 1015-1023.
Wang, N., Lee, I.J., Rask, G., and Wu, J.Q. (2016). Roles of the TRAPP-II Complex and the Exocyst in Membrane Deposition during Fission Yeast Cytokinesis. PLoS Biol *14*, e1002437.

Figure 1

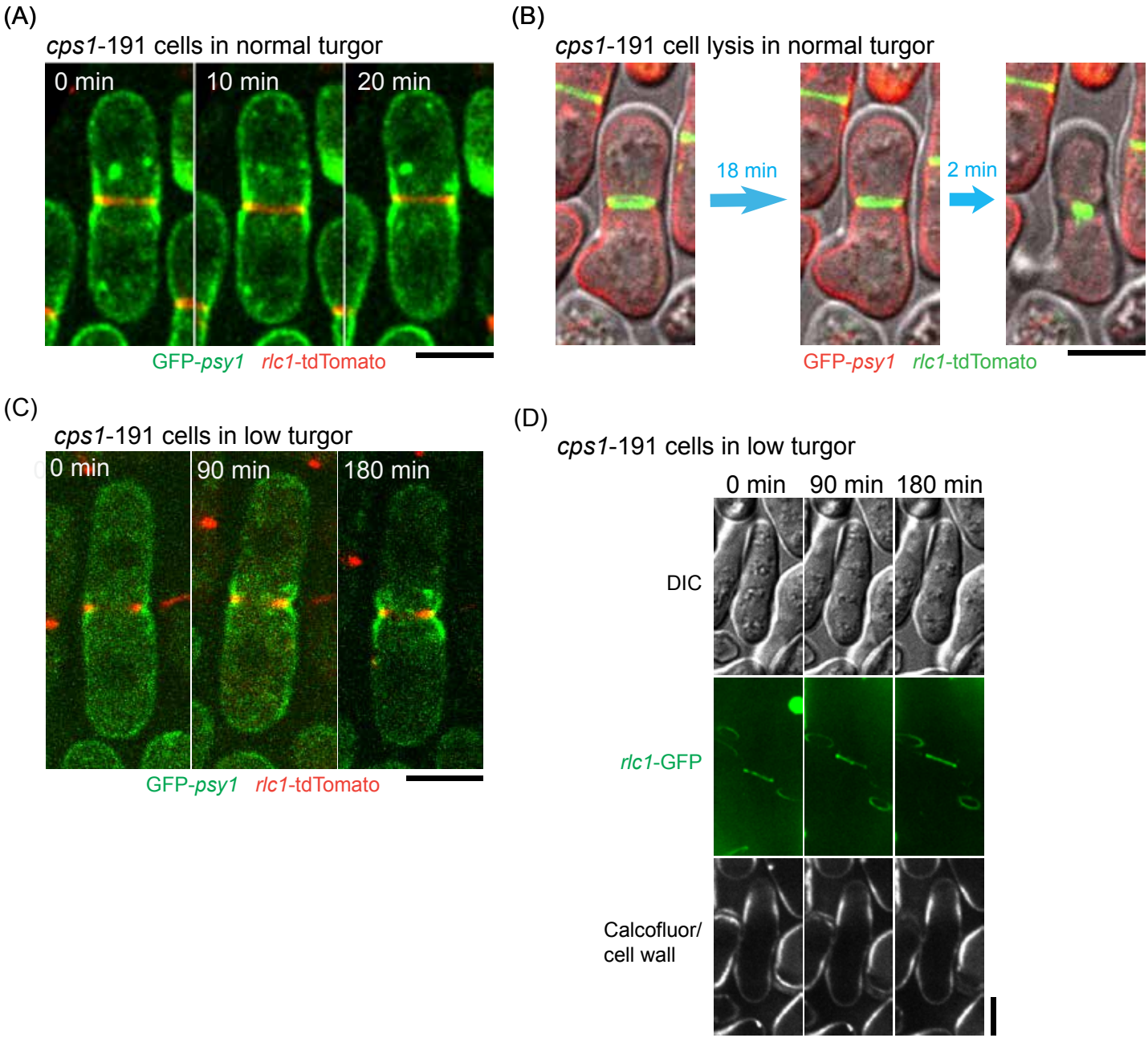
(A)
cps1-191 cells in normal turgor
0 min
10 min
20 min
GFP-*psy1* *rlc1*-tdTomato
(B)
cps1-191 cell lysis in normal turgor
18 min
2 min
GFP-*psy1* *rlc1*-tdTomato
(C)
cps1-191 cells in low turgor
0 min
90 min
180 min
GFP-*psy1* *rlc1*-tdTomato
(D)
cps1-191 cells in low turgor
0 min
90 min
180 min
DIC
rlc1-GFP
Calcofluor/
cell wall

Figure 2

(A) *cps1*-191 GFP-*psy1* *rlc1*-tdTomato

Spheroplast 1

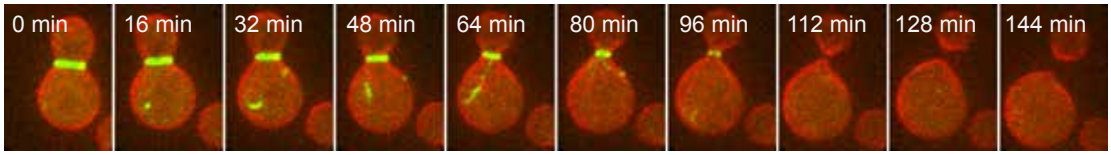

Spheroplast 2

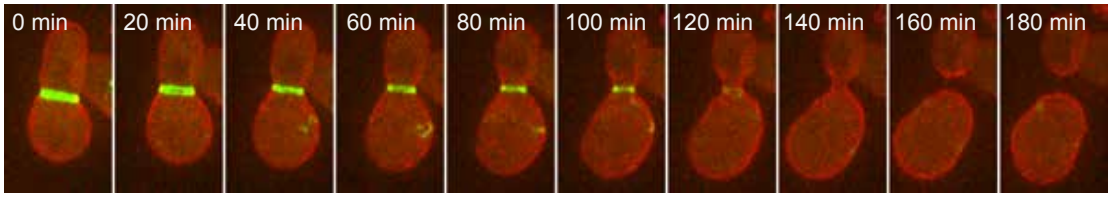

GFP-*psy1* *rlc1*-tdTomato

(B) *cps1*-191 *lifeact*-mCherry

Spheroplast 1

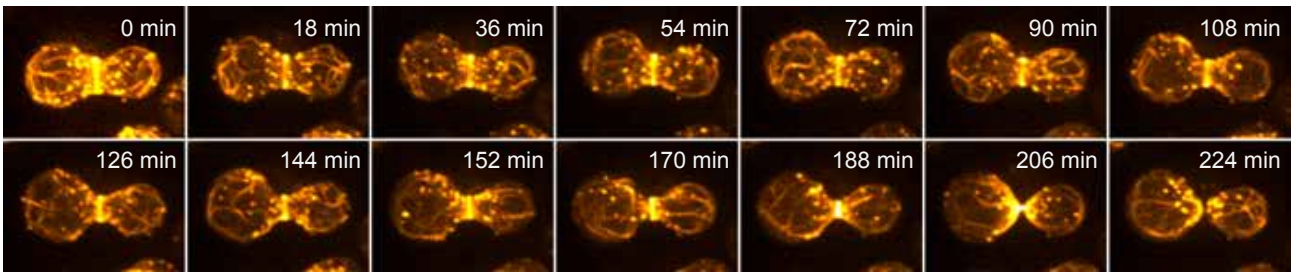

Spheroplast 2

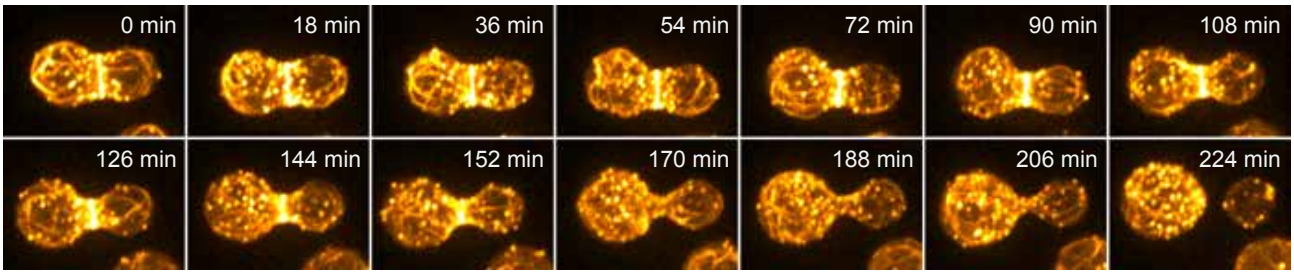

lifeact-mCherry

(C)

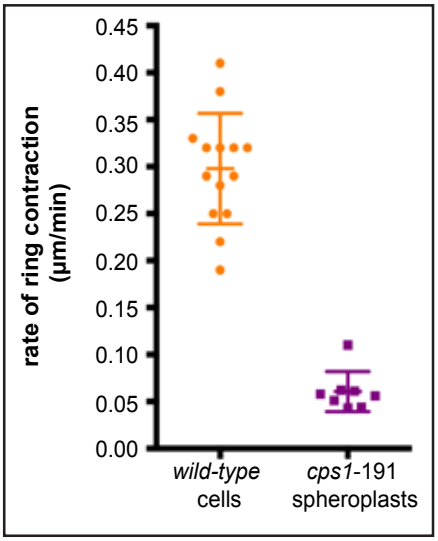

(D) DIC

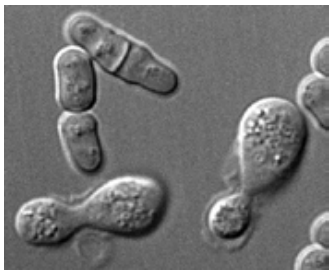

Calcofluor

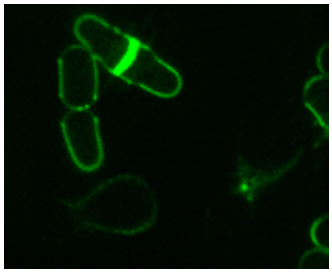

Wild-type cells + *cps1*-191 spheroplasts after 2h 50min in 2-DG medium

(E) In 2-DG medium

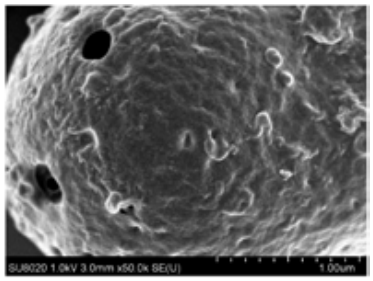

In medium without 2-DG

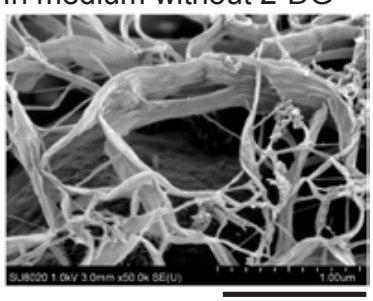

cps1-191 GFP-*psy1* *rlc1*-tdTomato

Figure 3

(A) *cps1*-191 *mok1*-664 GFP-*psy1* *rlc1*-tdTomato

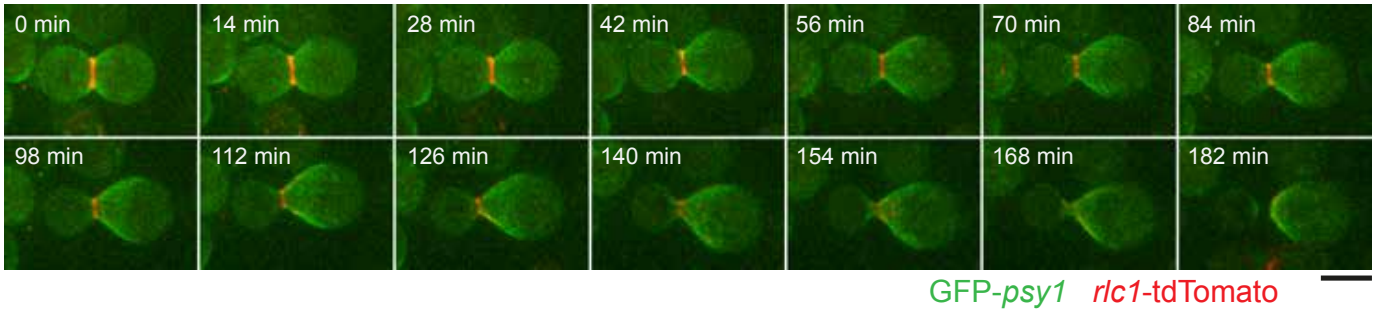

(B) *cps1*-191 *eng1*Δ GFP-*psy1* *rlc1*-tdTomato

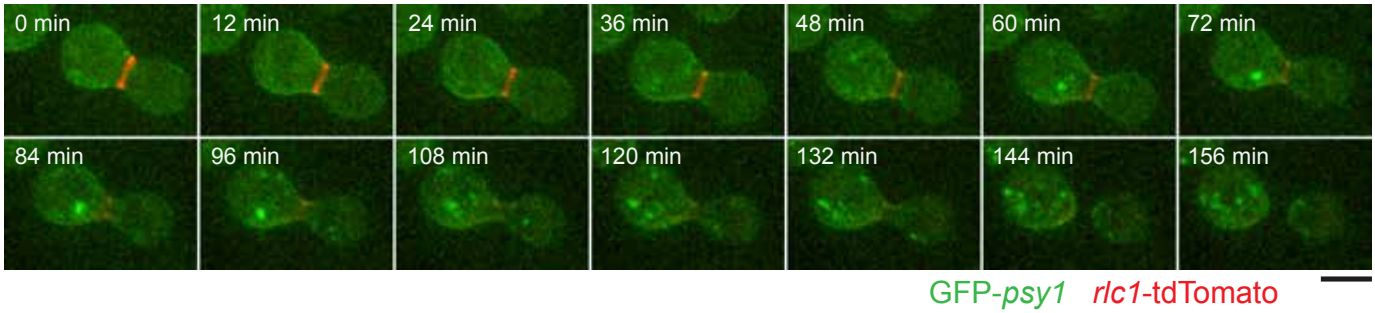

(C) *cps1*-191 *agn1*Δ GFP-*psy1* *rlc1*-tdTomato

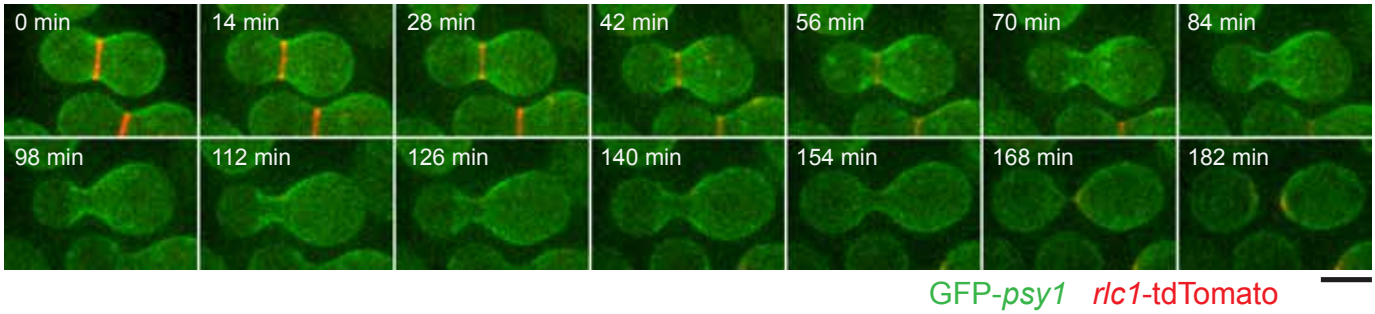

Figure 4

(A) *cps1*-191 GFP-*psy1* *rlc1*-tdTomato + DMSO

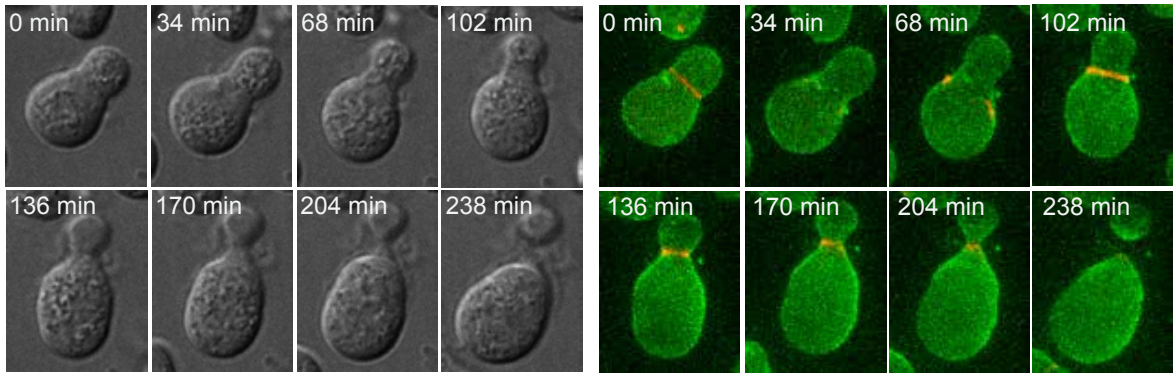

(B) *cps1*-191 GFP-*psy1* *rlc1*-tdTomato + Lat-A

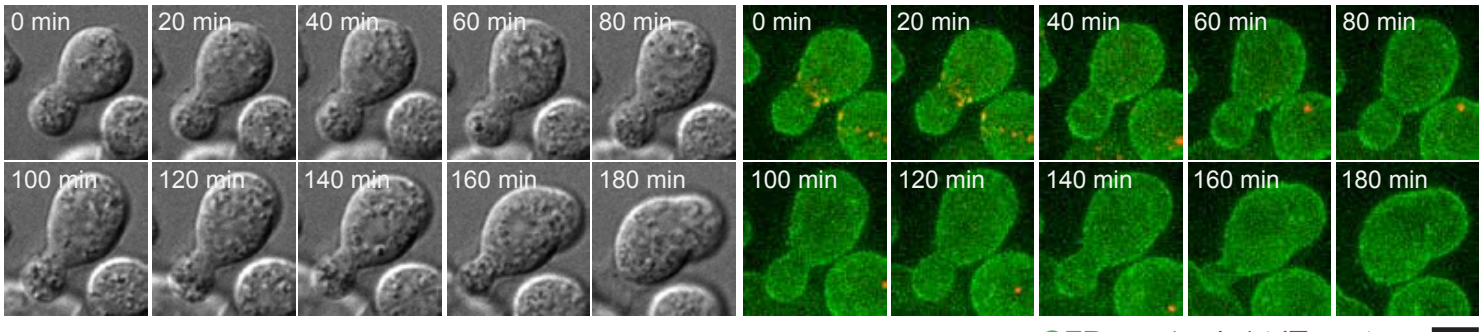

(C) *cps1*-191 *rlc1*Δ *cyk3*-GFP spheroplast

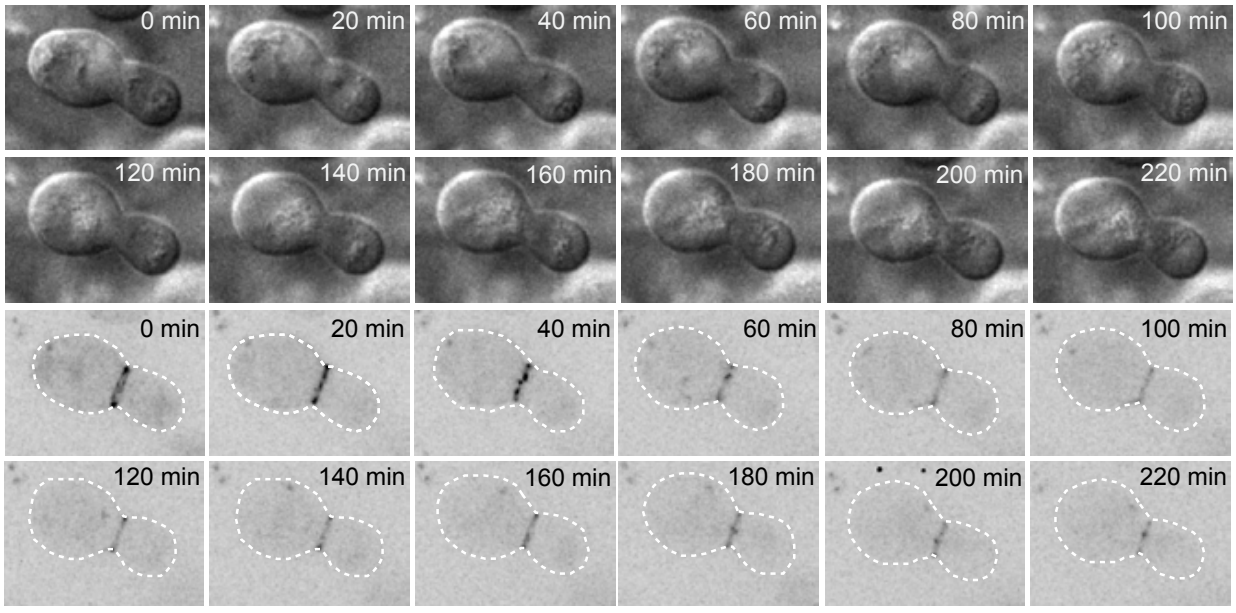

(D) *cps1*-191 GFP-*psy1* *rlc1*-tdTomato + Brefeldin A

Spheroplast 1

Spheroplast 2